Published in final edited form as:
J Control Release. 2012 June 28; 160(3): 561–569. doi:10.1016/j.jconrel.2012.04.005.

Microneedle delivery of plasmid DNA to living human skin: formulation coating, skin insertion and gene expression

Marc Pearton[1], **Verena Saller**[1], **Sion A Coulman**[1], **Chris Gateley**[2], **Alexander V Anstey**[2], **Vladimir Zarnitsyn**[3], and **James C Birchall**[1]

[1]School of Pharmacy and Pharmaceutical Sciences, Cardiff University, Redwood Building, King Edward VII Avenue, Cardiff, CF10 3NB, UK

[2]Aneurin Bevan Health Board, Royal Gwent Hospital, Cardiff Road, Newport, NP20 2UB, UK

[3]School of Chemical and Biomolecular Engineering, Georgia Institute of Technology, Atlanta, GA 30332, USA

Abstract

Microneedle delivery of nucleic acids, in particular plasmid DNA (pDNA), to the skin represents a potential new approach for the clinical management of genetic skin diseases and cutaneous cancers, and for intracutaneous genetic immunization. In this study excised human skin explants were used to investigate and optimize key parameters that will determine stable and effective microneedle-facilitated pDNA delivery. These include (i) high dose-loading of pDNA onto microneedle surfaces, (ii) stability and functionality of the coated pDNA, (iii) skin penetration capability of pDNA-coated microneedles, and (iv) efficient gene expression in human skin. Optimization of a dip-coating method enabled significant increases in the loading capacity, up to 100 micrograms of pDNA per 5-microneedle array. Coated microneedles were able to reproducibly perforate human skin at low (<1 Newton) insertion forces. The physical stability of the coated pDNA was partially compromised on storage, although this was improved through the addition of saccharide excipients without detriment to the biological functionality of pDNA. The pDNA-coated microneedles facilitated reporter gene expression in viable human skin. The efficiency of gene expression from coated microneedles will depend upon suitable DNA loading, efficient and reproducible skin puncture and rapid *in situ* dissolution of the plasmid at the site of delivery.

Keywords

Microneedle; coating; plasmid DNA; gene expression; human skin; skin puncture

1. Introduction

Microneedle (MN) devices dramatically increase the permeation of medicaments across the straum corneum (SC) for drug delivery applications in the skin [1]. The dimensions of microneedles are within the micron range and consequently their penetration, upon topical

Corresponding author: Dr J.C. Birchall, Reader in Pharmaceutics, School of Pharmacy and Pharmaceutical Sciences, Cardiff University, Redwood Building, King Edward VII Avenue, Cardiff, CF10 3NB, UK. Tel: +44 2920 875815, birchalljc@cf.ac.uk.

application, is restricted to the most superficial layers of the tissue i.e. the viable epidermis and papillary dermis [2]. MNs are therefore a minimally invasive, i.e. pain-free and patient-friendly, means of delivering a host of low molecular weight and macromolecular therapeutics into the skin and/or systemic circulation. MNs are produced using a range of manufacturing processes, including laser etching, silicon wet- and dry etching, integrated lens technology [3], polymer micromoulding and glass pulling, and from various materials including stainless steel, titanium, silicon, glass, polymers and carbohydrates [4]. The resulting MN devices display a diversity of geometries and physical properties with the mode of drug delivery being a function of the properties of the MNs. These delivery approaches fall into three broad categories: Firstly, the use of solid MNs to puncture the SC to transiently enhance the flux of a previously or subsequently applied topical formulation, e.g. solution, gel, cream, ointment, or transdermal patch. Secondly, the use of single or multiple hollow MNs to puncture the SC and provide a temporary physical conduit, i.e. the lumen of the needle, through which the drug can microinfuse into the skin. Finally, dry coating the drug formulation onto the surface of a solid MN [5] or incorporating the drug within the body of a degradable MN to facilitate both skin puncture and thereafter drug deposition following needle insertion and brief residence within the skin. Of these approaches, formulating medicament as a dry coat onto the surface of the MN has a number of particular advantages; solid MNs are simpler to manufacture than hollow or biodegradable MNs, a wide range of low and macromolecular therapeutics can be coated onto the MN surface and clinical usage would comprise a single administration step that could be potentially suited for self-administration. Furthermore the improved stability of the active material in a dried form could reduce the requirement for cold chain storage in the case of labile biomolecules and vaccines [6]. In many instances it would be advantageous to efficiently and reproducibly deliver nucleic acids to the skin epidermis. Plasmid and siRNA based therapies are being tested and clinically developed for the treatment of genetic skin disorders, cancers, wounds and hyper-proliferative diseases [7]. MNs may be particularity well suited for nucleic acid delivery, as they provide a means to deliver the polar macromolecular cargo across the lipid-rich SC barrier to specific localities and cellular populations within the skin. Delivering vaccines into the skin produces immune coverage that can be at least equivalent to, if not better than, that obtained via the subcutaneous or intramuscular routes, sometimes at reduced dose [8, 9, 10, 11, 12, 13]. This is due, in part, to the high density of antigen presenting cells (APCs) residing both within the epidermis and dermis, i.e. Langerhans cells (LCs) and dermal dendritic cells (DDCs) respectively.

DNA vaccines that rely on cellular transfection and subsequent expression of an encoded antigen possess a number of features that make them attractive alternatives to conventional inactivated or protein vaccines. For example, DNA vaccines could be particularly useful in pandemic situations, as plasmid manufacturing is relatively simple and rapid, plasmids are easy to manipulate and multiple antigens can be expressed from the same plasmid [14]. Plasmids are also relatively stable with a reduced requirement for cold chain storage, they are well tolerated by the patient, and no inactivation of pathogenic components is required [15]. In addition, specific motifs on the plasmid, regardless of the encoded antigen gene, can have immunomodulatory effects [16], causing the induction of LC migration [17] and a degree of adjuvancy. There is evidence that DNA vaccines physically delivered to the skin, for example smallpox DNA vaccine delivered via gene gun and MN-mediated electroporation [18], hepatitis C DNA vaccine dry coated onto MNs [5, 19] and herpes simplex virus type 2 (HSV-2) dry coated onto MNs [6], can provide robust protective immunity.

It is likely that a number of factors, both physical and biological, will influence the efficacy of pDNA delivered via coated microneedles [5, 19, 20]. The goal of this study is to consider some of these parameters including: loading capacity of pDNA onto MN surfaces, physical

and functional stability of MN-coated pDNA, the penetrative capability of uncoated and coated MNs and the level of gene expression in human skin following coated MN delivery. The degree of gene expression from coated MNs will thereafter be compared against a previously proven approach [21], i.e. applying a topical solution of pDNA to an area of skin that is subsequently treated with MNs.

2. Materials and methods

All reagents and laboratory consumables were purchased from Fisher Scientific UK, (Loughborough, UK), unless otherwise stated.

2.1 MN fabrication

The manufacturing process for the MNs used in this study has been detailed elsewhere [1, 2]. Briefly, MN designs were fabricated from 75 μm thick stainless steel sheets (Trinity Brand Industries, SS 304; McMaster-Carr, Atlanta, GA, USA) using an infrared laser (Resonetics Maestro, Nashua, NH, USA). The resultant planar MN arrays were electropolished prior to use.

2.2 MN penetration of human skin

Full thickness human skin (see Section 2.6) was removed from −20°C storage and allowed to defrost and equilibrate with the local environment. The subcutaneous fat was removed by blunt dissection and the skin mounted on a cork dissection board. Each MN design was manually inserted, perpendicular to the surface of the skin, for approximately 10 seconds before removal.

2.3 Histological examination of skin

Following MN treatment of skin approximately 50μl of 2% (w/v) methylene blue solution was applied by pipette. Excess solution was removed after 10 mins and the skin surface was swabbed with 70% ethanol. Skin was then rinsed in phosphate buffered saline (PBS) for 30 mins before fixation in 2% (v/v) glutaraldehyde for 2 hours at 4°C. Fixative was removed by two sequential 30 mins rinses in PBS. Skin was examined *en face* and images were captured using a Leica Zoom 2000 dissection microscope with an eyepiece digital camera. Treated skin samples were subsequently snap-frozen and 10μm histological sections were generated with a Leica cryomicrotome (Leica Microsystems (UK) Limited, Milton Keynes, UK). Sections were stained with hematoxylin and eosin, permanently mounted and examined by light microscopy.

2.4 Skin insertion force measurements

MNs were mounted in a bespoke adaptor that was connected to a 5N load cell (accuracy 0.4%), housed on a shortened Zwick Z0.5 materials testing machine (Zwick Testing Machines Ltd, Ulm, Germany). This enabled the maximum MN insertion force to be accurately controlled. Data were collected and processed using TestXpert II software (Zwick Testing Machines Ltd, Ulm, Germany). MNs were applied to *ex vivo* human skin at a constant insertion speed (10mm/min) and were programmed to retract from the tissue at a pre-determined force maxima. A range of maximum forces were evaluated (0.2, 0.5, 1.0, 1.5, 2.0, 2.5 and 3.0N). Methylene blue 2%w/v was applied to treated areas post-insertion and was removed from the skin surface after a contact time of 30 mins. To understand the influence of dry-coating on the mechanics of MN insertion uncoated, MNs (n=6) and dry-coated (100 immersions in 6mg/ml pCMVβ with 30 seconds drying time) MNs (n=6) were inserted into human skin to a maximum force of 2N and compared.

2.5 Dip-coating MNs with plasmid DNA (pDNA)

The dip-coating process used during these studies was based on a method developed by Gill and Prausnitz and has been described in detail elsewhere [5, 19]. Briefly, MNs are immersed into a formulation-loaded micro-coating station that is loaded with the relevant formulation and the MN is allowed to dry. This process is repeated in order to construct a layered coating on the MN surface.

2.5.1 Preparation of pDNA—The reporter plasmids pCMVβ and pEGFP-N1 were amplified and purified from previously transformed stocks of *E.coli* DH5α using antibiotic selective conditions and a QIAGEN Mega Kit (QIAGEN Ltd, Crawley, UK) [21].

2.5.2 Characterisation and optimisation of pDNA coating (light microscopy & electrophoresis)—The reservoir of the micro-dip coating device was loaded with a concentrated solution of pCMVβ (6 mg/mL). MNs were inserted into the coating station at a speed of approximately 2mm/second [5]. After each immersion the MN was retracted and allowed to air dry for either 5 or 30 seconds. This process was repeated for either 10, 40 or 100 sequential immersions. The coating station was refilled with 3–5 μL of plasmid solution on the completion of 20 immersions. The material coated onto the surface of each MN array was recovered in 150μL of a TE buffer rinsing solution. Aliquots were removed from the rinsing solution, loaded into a 2% agarose gel, supplemented with eithidium bromide, and subject to electrophoresis at 100 V for 1 hour.

2.5.3 Determination of time-dependent pDNA stability—The reservoir of the micro-dip coating device was loaded with a concentrated solution of pEGFP-N1 (6 mg/mL). Arrays of MNs (n=3) were coated using either 10 or 40 dips, with a 5 seconds drying time. Coated MNs were maintained at room temperature for 0, 1, 5 or 7 days. At each time-point coated material was recovered from the MN by reconstitution in 150 μL TE buffer and examined by electrophoresis, as described previously (Section 2.5.2).

2.5.4 Assessing pDNA functionality in vitro following microneedle coating—The biological functionality of the pDNA recovered from the pDNA stability experiment, described in Section 2.5.3, was ascertained by the transfection of cells *in vitro*. Five hundred nanograms of the recovered pDNA was diluted in 100 μL of OptiMEM I Reduced Serum Medium with 1.5 μL Lipofectamin LTX and 0.5 μL Plus Reagent (Life Technologies Ltd, Paisley, UK). The transfection complexes were added to HaCaT (Human adult low Calcium high Temperature keratinocytes) cells that had been cultured to 70% confluency. After 4 hours the media containing the transfection complexes was removed and the cells replenished with DMEM GlutaMAX™-I supplemented with 10% FBS and 2% Penicillin/ Streptomycin. After a further 44 hours of incubation at 37°C the cells were washed twice with chilled PBS, trypsinised (0.25% trypsin for 5 minutes at 37°C), collected, spun down for 2–3 minutes at 1000g and, after removal of the supernatant, resuspended in 200 μL of PBS. FACS analysis was performed on a FACSCalibur flow cytometer (BD Bioisciences, Oxford, UK), using Cell Quest v3.3 software (BD Bioisciences, Oxford, UK) and FlowJo v7.6.3 (Tree Star software, Ashland, OR, USA) post-analysis.

2.5.5 Incorporating sugars into the pDNA coating formulation—MNs were micro-dip coated, as described previously, with parameters of 10 dips and 5 seconds drying time between dips. The coating station reservoir was loaded with pCMVβ (5 mg/ml) alone or pCMVβ (5 mg/ml) supplemented with 1.5%w/v or 3%w/v of trehalose (Acros Organics), sucrose (Acros Organics) or maltose. Coated MNs were stored at room temperature for 7 days, after which coated material was recovered and examined by electrophoresis, as described previously (Section 2.5.2).

2.6 MN facilitated delivery of pDNA to viable human skin

The organ culture system used in this study is an adaptation of that used by Trowell and is described in detail elsewhere [22, 23]. Briefly, samples of human breast tissue were obtained from surgical procedures with full ethical committee approval and informed patient consent. Skin samples were transported from surgery to laboratory in 94% DMEM 25 mM HEPES supplemented with 5% FBS and 1% penicillin/streptomycin on ice and used within 2 hours of excision. Subcutaneous fat was removed by blunt dissection and the skin pinned out on a cork dissection board. Following MN treatment (Section 2.7) skin samples of approximately 1 cm^2 were incubated in organ culture at the air-liquid interface for 24 hours at 37°C, 5% CO_2.

2.7 Delivery of pDNA to human skin via dry coated MNs or topical solution

MNs coated with either the pEGFP-N1 (10 dips, 5 seconds drying time) or pCMVβ (40 dips, 30 seconds drying time) reporter plasmids were manually inserted into freshly excised human skin. MNs remained *in situ* for 10 mins before retraction. MN delivery of solutions of pDNA involved application of 10μl of 2mg/ml plasmid solution onto the skin surface prior to multiple penetrations of the skin using the MN device.

2.7.1 X-gal staining and histology—pCMVβ treated skin samples were X-gal stained to detect the β-galactosidase enzyme. Specimens were washed in PBS, supplemented with 4mM $MgCl_2$ (Sigma-Aldrich Company Ltd, Poole, UK), for 30 mins at room temperature. Each sample was fixed in 2% glutaraldehyde for 2 hours at 4°C, rinsed thoroughly in PBS/$MgCl_2$ and then immersed in X-gal staining solution maintained at 37°C for 24 hours. Following incubation samples were snap frozen in a dry ice/hexane bath, mounted with a Leica CM3035S cryostat where 10μm cryosections were generated.

2.7.2 Preparation of epidermal sheets and fluorescent microscopy—For pEGFP-N1 treated samples the epidermis was first isolated by incubating skin in 5ml of 3.8% ammonium thiocyanate at room temperature for 20–30 mins. The epidermis was removed from the dermis carefully with forceps under a dissection microscope. Isolated epidermis was mounted onto a slide and observed by fluorescent microscopy.

3. Results

3.1 MN characterization and penetration of human skin

The MNs used during these studies were 750μm in length and were arranged in an in-plane row of 5 microprojections (Fig. 1A). MN puncture of human skin was assessed using post penetration staining with methylene blue. Distinct regions of intense blue staining were observed *en face,* confirming that the stratum corneum had been breached (Fig. 1B). Examination of haematoxylin and eosin (H&E) stained cryosections revealed that the MNs penetrated the epidermis and extended into the papillary dermis (Fig. 1B). The depth of penetration was never more than 200μm, considerably shorter than the length of the MN (750μm). Methylene blue nuclear staining is clearly evident in epidermal cells radiating from the point of penetration and in nucleated dermal cells.

3.2 Skin insertion force measurements

Excised human skin was also used to analyse skin penetration as a function of the applied force of insertion. Following application of MNs to the skin surface, force displacement curves produced reproducible force-displacement profiles (Fig 2A). The force-displacement profile consists of two stages, an initial curved component followed by a straight line. The shape of the profiles that were evaluated was comparable, differing only in the extension of

the plot, which was determined by the maximum force. Post-penetration staining of the tissue (Fig 2B) revealed that MNs penetrated the skin at all of the insertion forces examined. However the diameter of the stained region (Fig 2C) was directly dependent upon the force of application, with the lowest forces (0.2N and 0.5N) producing significantly smaller regions of staining than the higher forces (3N).

3.3 Microcoating pDNA onto the surface of MNs

pDNA was coated onto the MNs using a previously described dip-coating method [5, 19]. The number of immersions into the pDNA reservoir and the intermediate drying time was adjusted to optimize the coating procedure (Fig. 3).

As expected, the quantity of plasmid coated onto the surface of the MNs increased upon an increased number of immersions. The mass of surface-coated pDNA also increased significantly ($p<0.01$) when the drying time between each MN immersion into the coating solution was increased from 5 seconds to 30 seconds (Fig. 3A). Following 100 immersions, each with a 30 second drying time, 105.7±22.9μg of pCMVβ was MN coated (approximately 20μg on each MN projection). The accumulation of coating on the MN surface after 10, 40 and 100 dips (using 30 seconds drying time) was also apparent when the coated MNs were visualised by light microscopy (Fig. 3C). Gel electrophoresis indicated that the signals attributed to supercoiled, open-circular and linear DNA increased in parallel as the number of immersions increased, the ratio of each band remaining relatively consistent, i.e. predominantly super-coiled DNA (Fig. 3B).

3.3.1 Force-displacement profiles for coated MNs—Investigations to determine the penetration capabilities of pDNA coated MNs (100 immersions in pDNA) indicated that although coating may slightly alter the mechanics of tissue penetration, the skin is nonetheless breached by the coated device. Force displacement curves for both coated and uncoated MNs (Fig. 4) have a comparable shape to previous profiles (Fig. 2), consisting of two characteristic sections, an initial curved component followed by a straight line. The data obtained for uncoated MNs were highly reproducible, resulting in a direct overlay of plots (n=6). For clarity, only a single representative plot is included for the uncoated MN in Fig. 4. Individual force displacement plots for coated MNs were distinguishable and therefore all plots are shown (Fig. 4). A comparison of the profiles reveals both similarities and differences between the penetration mechanics of coated and uncoated MNs. Uncoated MNs reached the straight line component of the plot after minimal displacement, <1mm, whereas the plots for coated MNs did not approach straight line behavior until a displacement of approximately 2mm. Interestingly, the gradient of the straight line component is comparable for all of the tested MNs, thus indicating that the relationship between force and displacement becomes directly proportional and independent of whether the microneeedles have been coated or not.

3.3.2 Stability and functionality of coated pDNA—The stability of pDNA following the dry-coating procedure was examined by gel electrophoresis (Fig. 5A). The physical stability of MN coated plasmid appears to decrease with storage, with the relative amount of supercoiled pDNA decreasing from approximately 80% to 50 % over 7 days storage. The biological functionality of the coated plasmid was determined by evaluating gene expression in HaCaT keratinocyte cells. Fig 5B shows that changes in the tertiary structure of the pDNA during the seven day storage period did not lead to a significant ($P>0.05$) reduction in expression of the reporter gene of pEGFP-N1.

Despite the retention of biological functionality, further studies aimed to determine whether the physical stability of MN coated pDNA could be enhanced. MNs were surface-coated (10

dips with 5 seconds drying time) with a formulation containing 5mg/ml pDNA plus a disaccharide at either 1.5% or 3% w/v. Figure I in the Online Supplement shows that addition of trehalose, sucrose or maltose to the coating formulation served to retain the tertiary physical structure of the stock plasmid (approximately 85% supercoiled) and that 1.5%w/v of disaccharide (15 mg/mL) was sufficient to achieve the stabilizing effect. The physical stability of the control sample, i.e. pDNA coated onto MNs in the absence of sugar, was commensurate with previous observations (Fig. 5A) with 58.1% of total pDNA in the supercoiled form after 7 days storage at room temperature.

3.4. MN facilitated delivery of pDNA to viable human skin

Freshly excised human skin was used to determine the biological functionality of MN delivered plasmid in the real human skin environment. Topical application of a solution of pCMVβ followed by MN puncture of the skin resulted in observable gene expression in the majority of treated *ex vivo* skin samples across a number of independent experiments. *En face* imaging illustrates discrete areas of exogenous gene expression in the skin (Fig. 6A) and subsequent review of transverse sections indicates that gene expression is confined to the viable epidermis at the site of MN penetration (Fig. 6C). Fluorescence imaging of an epidermal sheet, isolated from full thickness human skin that had been treated with pEGFP-N1 plasmid also supports suggestions that the expression of pDNA is proximal to the MN application site (Fig. 6B).

Insertion of pDNA-coated MNs into viable human skin for 10 min also resulted in positive gene expression (Fig. 7), albeit at statistically ($P<0.01$) reduced levels when compared to topical liquid application of the plasmid in combination with MN puncture (Figure 8). Discrete areas of gene expression were observed following delivery of the dried pDNA formulation (Fig. 7A&B) and, in a comparable manner to liquid pDNA application (Fig. 6), gene expression was confined to the viable epidermis at the site of MN puncture (Fig. 7B&C).

4. Discussion

An effective nucleic acid delivery system that can induce protein synthesis in the skin has many potential clinical applications, including genetic immunisation. The primary aim of this study was to evaluate the potential of a dry-coated microneedle delivery system as a means to facilitate the expression of exogenous pDNA in the human epidermis.

Effective and reproducible microneedle-assisted delivery in the clinical setting will be dictated, in part, by predictable and reliable skin penetration. Further work is therefore required to determine the influence of microneedle parameters and application forces on the penetration of human skin. Whilst a definitive evaluation of the mechanics of MN insertion is required, in this study we performed a small number of informative experiments to provide confidence that the microneedles used in this study are able to penetrate skin effectively and deliver the material to the underlying viable epidermis. Penetration of the MN array into excised human skin was achieved with forces as low as 0.2N, which equates to just 0.04N per MN. These insertion forces were comparable with those observed in previous studies [24, 25]. Increasing the insertion force results in greater skin disruption and hence an increase in the permeation of soluble compounds such as methylene blue. In these experiments the mechanics of MN puncture are captured by two distinct phases, as shown in the force-displacement curves generated through microneedle insertion. The first stage is an upward curved trajectory from 0mm to a distance of approximately 2mm; this characterises two events. The first event is loading deformation, whereby the MN contacts the skin surface and causes deformation of the skin during the downward application of the device. This is comparable to the first phase of hypodermic needle insertion [26, 27]. The second

event is penetration of the tissue by the sharp MN tip. During penetration of a hypodermic needle [26, 27] rupture of the skin surface is captured by a brief downward deflection of the force-displacement curve. However the radius of curvature for MN tips is considerably smaller than that of hypodermic needles, thus enabling the MN to progressively cut into the SC at the micron scale. Although rupture events were noted in a previous study of microneedle penetration in human skin [24], significant rupture events were not observed during our studies.

En face imaging suggests that MN penetration of the tissue begins at forces as low as 0.2N. The small diameters of the stained microdisruptions suggest that at this force the needle tip begins to penetrate into the tissue. However as downward displacement continues an increasing proportion of the tapered needle tip makes contact with the SC, resulting in a greater contact area between the MN and the tissue. This results in an exponential increase in the resistive forces between the needle and the tissue, thus explaining the curved nature of the force-displacement plot observed between 0mm and approximately 2mm (force measurements up to approximately 1.5N). *En face* imaging supported these results, indicating that gradual insertion of the MN causes progressive widening of the microdisruption (up to 1.5N) as the tip of the MN progressively cuts into the skin.

The second stage of the penetrative process is dominated by entrance of the MN shaft into the skin. The frictional forces of the tissue on the shaft do not appear to have a significant impact on the recorded force, which continues to be dictated by the resistive forces at the MN tip. Therefore after a displacement of approximately 2mm (and a resistive force of approximately 2N) the force-displacement curve continued in a relationship that is almost directly proportional i.e. a straight line. *En face* images confirm this, as the MN shaft enters the skin the diameter of the surface microdisruption does not increase significantly. However the depth of the created microchannel would inevitably extend into the underlying tissue and thus would facilitate delivery of a pDNA formulation to the epidermal cells beneath the stratum cornuem.

Sequential micro-dip coating was used to load the MN surface with pDNA. Following 40 dips into the coating solution the pDNA appeared to deposit around the centre of the MN shaft. However, as the number of dips was increased the coated material collected towards the base of the MN. Whilst this deposition pattern may create a problem, as the entire coating would not deposit even if the MN were fully inserted, conversely it may also be advantageous if the aim is to target much of the coated material to the viable epidermis. In the context of DNA vaccination, the viable epidermis is the target region, given the high density of metabolically active keratinocytes capable of expressing exogenous genes and the dense population of resident LCs. Clearly, the MN coating strategy is likely to be dependent on the intended application and is also likely to be a compromise between sufficient drug loading, efficient skin insertion and complete and targeted deposition of the payload. Through simple modification of the dip-coating procedures and conditions we were able to coat up to 100 micrograms of pDNA per 5 needle array. This is an order of magnitude higher than the nanogram quantities of pDNA that have been loaded onto microneedles in previous studies [28, 29] and most likely reflects greater optimisation of the concentration of the pDNA coating formulation, increased immersions into the formulation and an extended intermediate drying time.

MNs that were extensively coated with pDNA (100 dips) were still able to penetrate the skin effectively, displaying similar insertion mechanics to uncoated microneedles. The initial curved phase of the insertion force displacement graph was however shallower for the coated MNs. Therefore, coated MNs experience a resistive force of 2N after approximately 2mm displacement, whereas uncoated MNs experience this resistive force after

approximately 1.5mm. This can be explained by the ability of the MNs to penetrate the tissue. We might expect the uncoated MN to initiate penetration of the SC more easily than the MN tip that has been coated in pDNA. Therefore, for the uncoated MN, resistive forces are brought to action quickly over the entire area of the bevelled MN tip. However, the less sharp tip of coated MNs may result in delayed penetration, greater deflection of the tissue on initial contact and thus the displacement required to insert the entire MN tip into the skin will be greater. However, once the needle tip is entirely immersed in the skin frictional forces on the shaft of coated and uncoated MNs are analogous, as demonstrated by the equivalent gradients in the linear portion of the force displacement curves. Ultimately, although there were small differences in the biomechanics of the initial stages of skin penetration, both uncoated and dry-coated MNs were able to successfully penetrate human skin with relative ease. Whilst the application of microneedles to different treatment sites in a single human donor has indicated acceptable levels of intra-individual variability and provided confidence that reproducible pDNA delivery could be achieved, the influence of inter-individual variability has not been addressed. More extensive studies to examine the penetration of human skin by a range of MN morphologies, at a range of forces, in a variety of donor tissues, from different skin sites are required to produce definitive and comprehensive information regarding the mechanics of microneedle penetration. This would guide the development of microneedle designs and applicator systems for pDNA and other therapeutics.

Retaining the physical, chemical and biological stability of the material coated onto the MN represents a more substantial challenge. Gel electrophoresis of recovered pDNA showed a noticeable change in pDNA tertiary structure when the coated MNs were stored over one week. Interestingly, the reduction in supercoiled pDNA fraction was more exaggerated in pDNA recovered from MNs coated with 10 dips when compared with those coated with 40 dips. Speculating why this may be the case, in 10-dip samples a higher relative proportion of the coated pDNA is exposed either to the metal/liquid interface or the air/liquid interface which could modestly amplify the adverse effect of any oxidative instability caused by the metallic MN surface and/or the external environment [30, 31]. The addition of simple sugar excipients into the coating formulation served to reduce pDNA degradation in the 10-dip samples over 7 days storage. Such sugars are commonly used in pharmaceutical formulations to prevent damage to macromolecular structures during freezing, drying and storage [32].

Changes in the tertiary structure of the pDNA on storage did not appear to reduce the gene expression efficiency of the plasmid in cultured cells. As the reduction in supercoiled fraction did not influence gene expression, it may be assumed that cleavage of the pDNA occurs at a location that does not affect cell transfection or GFP expression in HaCaT cells. It is also possible however that the amount of pDNA used in the cell transfection study was excessive and therefore subtle functional changes to the plasmid could not be observed.

Subsequent studies in viably maintained excised human skin have demonstrated reporter gene expression when pDNA was delivered via MNs. Gene expression was restricted to cells within the viable epidermis and always in the direct vicinity of a MN channel. Interestingly, although the level of exogenous gene expression can be variable in skin explants, reporter gene expression appeared to be more consistent and more intense in control samples whereby a solution of pDNA was applied to the skin followed by MN application. In these samples a total of 20μg of pDNA in solution is applied to the skin surface before microporating skin with uncoated microneedles. Therefore the mass of pDNA delivered under the stratum corneum is likely to be in the nanogram range, an order of magnitude less than the coated microneedles whereby microgram quantities of pDNA are

deposited into the epidermis/dermis. Our laboratory has considerable experience in the delivery of pDNA using microneedle devices [21, 22] and this is not an isolated observation.

In this study consecutive immersions of the MN device in a pDNA solution produced a dry coat of pDNA on the microneedle tip and shaft. To facilitate cellular delivery of the pDNA upon/following MN application it is imperative that a sufficient volume of solvent is available to facilitate dissolution i.e. the environment proximal to the MN must possess enough water to permit rapid dissolution of the pDNA from the microneedle. If an appropriate volume is not available the payload will either remain on the MN or, more likely, be deposited in the skin as a solid pDNA pellet. Therefore we should consider the fate of the pDNA formulation following deposition into the skin.

Dissolution of pDNA is a common laboratory procedure for those researchers involved in nucleic acid based research e.g. pDNA extraction from a transformed bacteria. During these laboratory procedures a pDNA concentration of 1mg/ml is often selected as a reasonable storage and usage concentration [21]. However to obtain this concentration, the dissolution process for a pDNA pellet often requires gentle agitation and extended time periods. Additionally, over-drying a pDNA pellet can often hamper dissolution.

Therefore when considering MN facilitated delivery of a dry-coated pDNA formulation, let us presuppose a coating of 4 μg of pDNA over a single entire MN and also assume that complete dissolution of the pDNA may require a volume of 4μL water. If we simplify the microneedle and consider it to be a rectangular cuboid of dimension 700μm × 200μm × 75μm, its volume would be $0.0105mm^3$ (0.0105 μL). Therefore the volume of water needed to dissolve the pDNA coating (4μL) would be approximately four hundred times greater than the needle volume. The water available in the skin for dissolution of a dry-coated formulation is complicated by the heterogenous structure of the stratified tissue and the complexity of the biological environment. However we know that the environment proximal to the microneedle, the epidermis and dermis, not only consists of water but also a diversity of lipid and protein-based biological structures and we also know that much of the water in the skin is bound [33]. Therefore, although intra- and inter- individual differences in water content have been acknowledged [34, 35, 36], it is not unreasonable to approximate the water available for dissolution to be approximately 50% of the environment surrounding the microneedle. This suggests that a skin volume of $8mm^3$ (8μl) would contain sufficient moisture to facilitate dissolution of pDNA from a single microneeedle, a volume that is 800 times greater than the microneedle volume (see Figure II in the Online Supplement). The absence of a mixing mechanism, i.e. agitation, also means that a high pDNA concentration is likely to be maintained in the immediate environment surrounding the MN, thus hampering diffusion of the pDNA into the bulk phase. This has led us to propose that dissolution of extensively dry-coated pDNA formulations may be a protracted process.

If pDNA dissolution were delayed, this may explain the difference in the gene expression efficiencies associated with dry-coated versus liquid pDNA formulations. We hypothesise that pDNA uptake into the viable cells of the epidermis is assisted by transient disruptions in tightly packed kerationocytes during microneedle insertion. Indeed, previous studies using the topical pDNA solution approach suggested that skin puncture with frustum tipped MNs results in greater exogenous gene expression than sharp tipped MNs due to the heightened level of tissue disruption caused by the frustum designs [37]. This hypothesis is also supported by restricted expression of the exogenous pDNA in the cellular region proximal to microneedle disruption (Fig. 6). We postulate that the mechanism of microneedle-mediated cellular uptake of an aqueous pDNA formulation is an almost instantaneous process i.e. microneedles introduce pDNA into the aqueous environment of the viable epidermis, cell membranes are temporarily disrupted by the microneedle insertion event and, during the

rapid re-organisation of the cell membranes to restore integrity, pDNA is able to diffuse into the intracellular space (see Fig. 9). If this is the case, whereas pDNA that is already in solution will be able to exploit these transient delivery pathways, pDNA delivered in dry form may not dissolve rapidly enough to take advantage of the temporary disruption in cell integrity. The hypothesis also explains why pDNA can effectively transfect keratinocytes in live tissue without using the non-viral/viral gene transfer vectors that are required to facilitate *in vitro* transfection of immortalised cell lines.

It should of course be noted that these observations are particular to pDNA delivery via extensively coated microneedles whereby cell uptake appears to be intimately affected by pharmaceutical form and spatial/temporal factors. Microneedle delivery of other molecules, macromolecules and particulates are not influenced by such factors. It should also be noted that our observations may be unique to the human skin model we employ. Indeed, previous studies have demonstrated positive gene expression in skin following delivery of pDNA coated onto microneedles [29, 38]. It is important to stress however that these studies looked at the functional endpoint (such as improved immune response from a DNA vaccine), which does not necessarily result from localised gene expression in epidermal cells. Such studies have also employed animal models and hence acknowledged differences in the physiology of animal and human skin and also differences in the location of pDNA deposition may explain disparate results.

5. Conclusions

In summary, in this study we have been able to coat considerable quantities of pDNA onto steel microneedles, demonstrate satisfactory stability of the coating and insignificant adverse effects on microneedle penetration. The coated pDNA dissolves from the microneedle *in situ* and is capable of expressing the gene product local to the microneedle puncture in the epidermis of viable human skin. Given the clear advantages of improved dose-loading, enhanced physical/chemical stability and ease of application using this delivery method, further work is now warranted to optimise the degree and nature of the nucleic acid coating to encourage rapid dissolution for enhanced gene expression efficiency.

Supplementary Material

Refer to Web version on PubMed Central for supplementary material.

Acknowledgments

This work was funded by the National Institutes of Health Grant EB006369.

References

1. Prausnitz MR. MNs for transdermal drug delivery. Adv Drug Deliv Rev. 2004; 56(5):581–587. [PubMed: 15019747]
2. Coulman SA, Birchall JC, Alex A, Pearton M, Hofer B, O'Mahony C, Drexler W, Povazay B. In vivo, in situ imaging of MN insertion into the skin of human volunteers using optical coherence tomography. Pharm Res. 2011; 28:66–81. [PubMed: 20464461]
3. Park JH, Yoon YK, Choi SO, Prausnitz MR, Allen MG. Tapered conical polymer microneedles fabricated using an integrated lens technique for transdermal drug delivery. IEEE T Bio-Med Eng. 2007; 54(5):903–13.
4. Donnelly RF, Raj Singh TR, Woolfson AD. Microneedle-based drug delivery systems: microfabrication, drug delivery, and safety. Drug Deliv. 2010; 17(4):187–207. [PubMed: 20297904]
5. Gill HS, Prausnitz MR. Coated MNs for transdermal delivery. J Control Release. 2007; 117(2):227–237. [PubMed: 17169459]

6. Kask AS, Chen XF, Marshak JO, Dong LC, Saracino M, Chen D, Jarrahian C, Kendall MA, Koelle DM. DNA vaccine delivery by densely-packed and short microprojection arrays to skin protects against vaginal HSV-2 challenge. Vaccine. 2010; 28:7483–7491. [PubMed: 20851091]
7. McLean WH, Moore CB. Keratin disorders: from gene to therapy. Hum Mol Genet. 2011; 20(R2):R189–97. [PubMed: 21890491]
8. Kim YC, Quan FS, Yoo DG, Compans RW, Kang SM, Prausnitz MR. Improved influenza vaccination in the skin using vaccine coated MNs. Vaccine. 2009; 27(49):6932–6938. [PubMed: 19761836]
9. Koutsonanos DG, del Pilar Martin M, Zarnitsyn VG, Sullivan SP, Compans RW, Prausnitz MR, Skountzou I. Transdermal influenza immunization with vaccine-coated MN arrays. PLoS One. 2009; 4(3):e4773. [PubMed: 19274084]
10. Song JM, Kim YC, Lipatov AS, Pearton M, Davis CT, Yoo DG, Park KM, Chen LM, Quan FS, Birchall J, Donis RO, Prausnitz MR, Compans RW, Kang SM. MN delivery of H5N1 influenza virus-like particles to the skin induces long-lasting B and T cell responses in mice. Clin Vaccine Immunol. 2010; 17(9):1381–1389. [PubMed: 20631330]
11. Zhu Q, Zarnitsyn VG, Ye L, Wen Z, Gao Y, Pan L, Skountzou I, Gill HS, Prausnitz MR, Yang C, Compans RW. Immunization by vaccine-coated MN arrays protects against lethal influenza virus challenge. Proc Natl Acad Sci USA. 2009; 106(19):7968–7973. [PubMed: 19416832]
12. Fernando GJP, Chen X, Prow TW, Crichton ML, Emily JF, Roberts MS, Frazer IH, Brown LE, Kendall MAF. Potent immunity to low doses of influenza vaccine by direct delivery to immune cells in skin. PLoS One. 2010:e10266. [PubMed: 20422002]
13. Fernando GJP, Chen X, Primiero CA, Yukiko EJ, Fairmaid SR, Corbett HJ, Frazer IH, Brown LE, Kendall MAF. Nanopatch targeted delivery of both antigen and adjuvant to skin synergistically drives enhanced antibody responses. Journal of Controlled Release. 2012 In Press. 10.1016/j.jconrel.2012.01.030
14. Phillips AJ. The challenge of gene therapy and DNA delivery. J Pharm Pharmacol. 2001; 53(9): 1169–1174. [PubMed: 11578098]
15. Patil SD, Rhodes DG, Burgess DJ. DNA-based therapeutics and DNA delivery systems: A comprehensive review. The AAPS J. 2005; 7(1):E61–77.
16. Cornelie S, Poulain-Godefroy O, Lund C, Vendeville C, Ban E, Capron M, Riveau G. Methylated CpG-containing plasmid activates the immune system. Scand J Immunol. 2004; 59(2):143–151. [PubMed: 14871290]
17. Ban E, Dupre L, Hermann E, Rohn W, Vendeville C, Quatannens B, Ricciardi-Castagnoli P, Capron A, Riveau G. CpG motifs induce Langerhans cell migration in vivo. Int Immunol. 2000; 12(6):737–745. [PubMed: 10837401]
18. Hooper JW, Golden JW, Ferro AM, King AD. Smallpox DNA vaccine delivered by novel skin electroporation device protects mice against intranasal poxvirus challenge. Vaccine. 2007; 25(10): 1814–1823. [PubMed: 17240007]
19. Gill HS, Prausnitz MR. Coating formulations for microneedles. Pharm Res. 2007; 24(7):1369–1380. [PubMed: 17385011]
20. Romani N, Thurnher M, Idoyaga J, Steinman RM, Flacher V. Targeting of antigens to skin dendritic cells: possibilities to enhance vaccine efficacy. Immunol Cell Biol. 2010; 88(4):424–430. [PubMed: 20368713]
21. Birchall JC, Coulman SA, Pearton M, Allender C, Brain K, Anstey A, Gateley C, Wilke N, Morrissey A. Cutaneous DNA delivery and gene expression in ex vivo human skin explants via wet-etch microfabricated microneedles. J Drug Target. 2005; 13(7):415–421. [PubMed: 16308210]
22. Ng KW, Pearton M, Coulman SA, Anstey A, Gateley C, Morrissey A, Allender C, Birchall J. Development of an ex vivo human skin model for intradermal vaccination: Tissue viability and Langerhans cell behaviour. Vaccine. 2009; 27(43):5948–5955. [PubMed: 19679220]
23. Trowell OA. A modified technique for organ culture in vitro. Exp Cell Res. 1954; 6:246–248. [PubMed: 13142005]

24. Davis SP, Landis BJ, Adams ZH, Allen MG, Prausnitz MR. Insertion of microneedles into skin: measurement and predictionn of insertion force and needle fracture force. J Biomech. 2004; 37(8): 1155–1163. [PubMed: 15212920]
25. Yang M, Zhan JD. Microneedle insertion force reduction using vibratory actuation. Biomed Microdevices. 2004; 6(3):177–182. [PubMed: 15377826]
26. Nguyen CT, Vu-Khanh T. Mechanics and mechanisms of puncture by medical needles. Procedia Engineering. 2009; 1(1):139–42.
27. Mahvash M, Dupont PE. Mechanics of dynamic needle insertion into a biological material. IEEE T Bio-Med Eng. 2010; 57(4):934–943.
28. Gill HS, Söderholm J, Prausnitz MR, Sällberg M. Cutaneous vaccination using microneedles coated with hepatitis C DNA vaccine. Gene Ther. 2010; 17(6):811–814. [PubMed: 20200562]
29. Gonzalez-Gonzalez E, Speaker T, Hickerson R, Spitler RP, Flores MA, Leake D, Contag CH, Kaspar RL. Silencing of reporter gene expression in skin using siRNAs and expression of plasmid DNA delivered by a soluble protrusion array device (PAD). Mol Ther. 2010; 18(9):1667–1674. [PubMed: 20571543]
30. Evans RK, Xu Z, Bohannon KE, Wang B, Bruner MW, Volkin DB. Evaluation of degradation pathways for plasmid DNA in pharmaceutical formulations via accelerated stability studies. J Pharm Sci. 2000; 89(1):76–87. [PubMed: 10664540]
31. Hong J, Lee E, Carter JC, Masse JA, Oksanen DA. Antioxidant-accelerated oxidative degradation: a case study of transition metal ion catalyzed oxidation in formulation. Pharm Dev Technol. 2004; 9(2):171–179. [PubMed: 15202576]
32. Colaço C, Sen S, Thangavelu M, Pinder S, Roser B. Extradinary stability of enzymes dried in trehalose: simplified molecular biology. Nat Bio. 1992; 10:1007–1011.
33. Gniadecka M, Nielsen OF, Christensen DH, Wulf HC. Structure of water, proteins, and lipids in intact human skin, hair, and nail. J Invest Dermatol. 1998; 110:393–398. [PubMed: 9540981]
34. Potts RO, Buras EM Jr, Chrisman DA Jr. Changes with age in the moisture content of human skin. J Invest Dermatol. 1984; 82:97–100. [PubMed: 6690633]
35. Madison KC. Barrier functions of the skin: “La Raison d’Être” of the epidermis. J Invest Dermatol. 2203; 121(2):231–241. [PubMed: 12880413]
36. Warner RR, Myers MC, Taylor DA. Electron probe analysis of human skin: determination of the water concentration profile. J Invest Dermatol. 1988; 90:218–224. [PubMed: 3339263]
37. Pearton M, Allender C, Brain K, Anstey A, Gateley C, Wilke N, Morrissey A, Birchall J. Gene Delivery to the Epidermal Cells of Human Skin Explants Using Microfabricated Microneedles and Hydrogel Formulations. Pharm Res. 2008; 25(2):407–416. [PubMed: 17671832]
38. Gill HS, Söderholm J, Prausnitz MR, Sällberg M. Cutaneous vaccination using microneedles coated with hepatitis C DNA vaccine. Gene Ther. 2010; 17:811–814. [PubMed: 20200562]

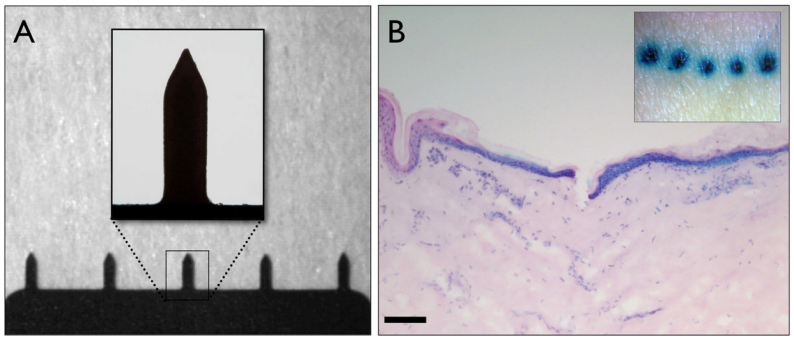

Figure 1. Microneedle morphology and skin penetrative capabilities

(A) Bright field micrographs of an in-plane row of five microneedles, each with a height of approximately 750μm, insert shows in greater detail the microneedle geometry. (B) *En face* (insert) and 10μm H&E stained histological section of human skin treated with microneedles and post-stained with methylene blue (bar = 300μm).

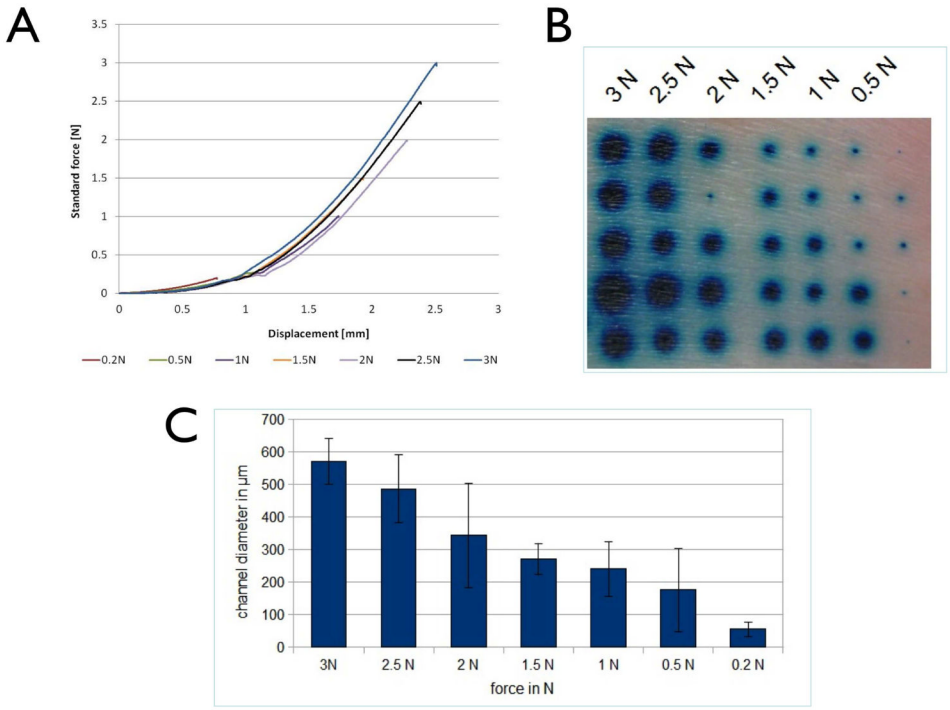

Figure 2. Application force required for skin penetration

(A) Force displacement curves generated during the application of microneedles to excised human skin. Force-displacement profiles were recorded for all microneedle applications (0.2–3N), up to a maximum force of 3N. (B,C) Methylene blue post-staining showing degree of skin penetration following microneedle application. (B) *En face* visualization of staining following skin puncture with varying force. (C) Quantification of lateral diffusion of the dye correlates microneedle application force with degree of skin penetration. Data presented as mean ± SD.

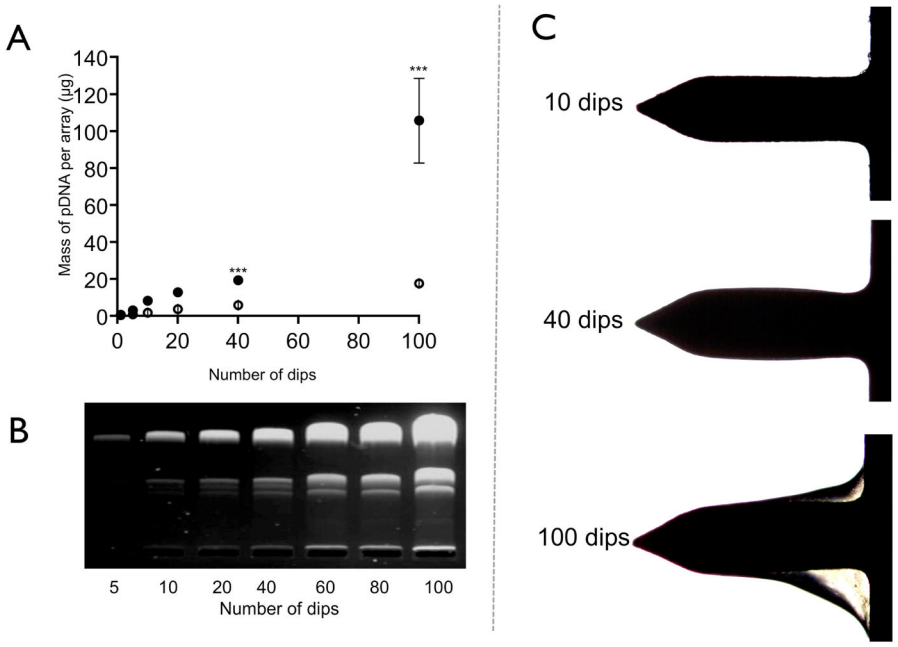

Figure 3. Microneedles dip-coated coated with pDNA

(A) UV-spectrophotometric quantification of pDNA dip-coated onto microneedles with increasing number of dips and varying drying time from 5 seconds (open circles) to 30 seconds (closed circles). Data presented as mean ± SD (n=4); One way analysis of variance, ***P < 0.01. (B) Gel electrophoresis of pDNA recovered from microneedles following surface coating with varying number of dips (30 seconds drying time). (C) Bright field micrographs showing the build up of pDNA on the surface of the microneedles when the number of dips was increased (30 seconds drying time).

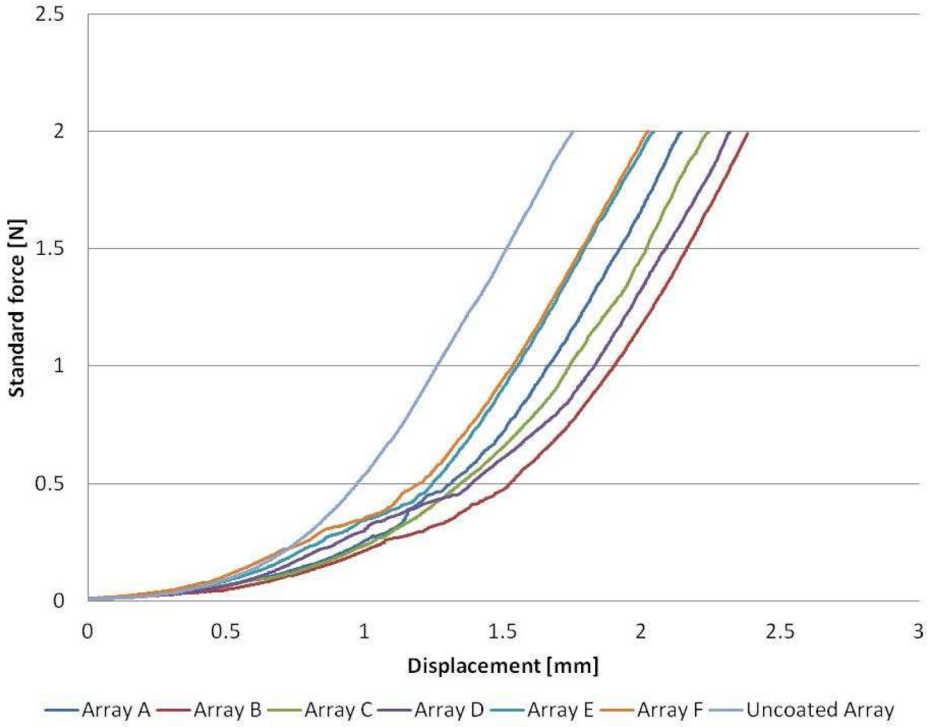

Figure 4. Force displacement during coated and uncoated microneedle insertion

Force displacement profiles comparing both coated (Arrays A – F) and uncoated MN devices.

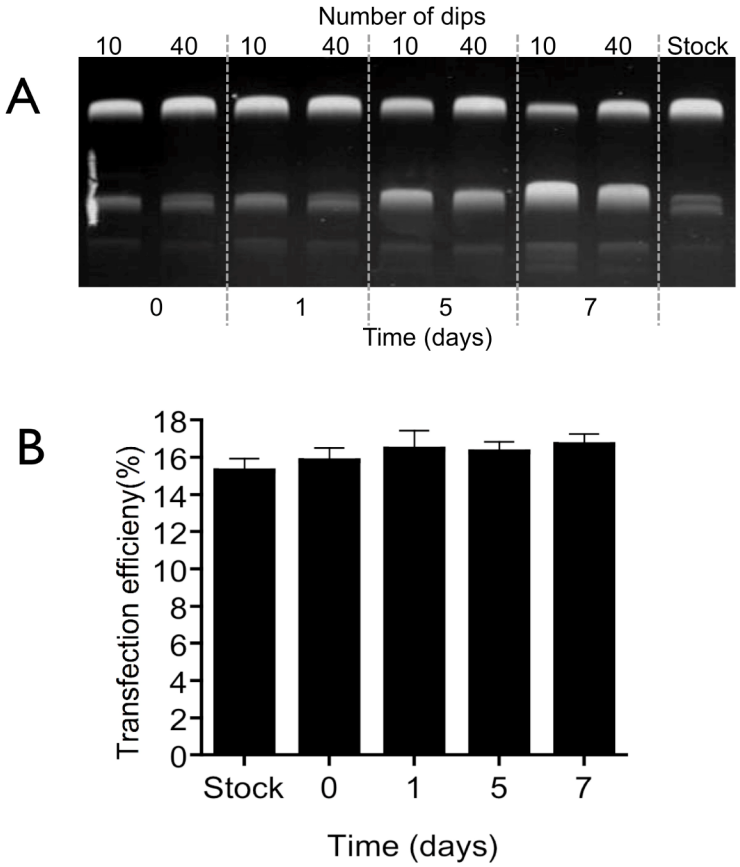

Figure 5. Stability and functionality of surface-coated pDNA

(A) Gel electrophoresis of pDNA coated with either 10 or 40 dips (5 seconds drying time) recovered over a period of 7 days. (B) HaCaT cell transfection efficiency as determined by flow cytometry using recovered pDNA (pEGFP) surface-coated onto microneedles for 1, 5, or 7 days. Data presented as mean ± SD (n=4); One way analysis of variance, $P > 0.05$.

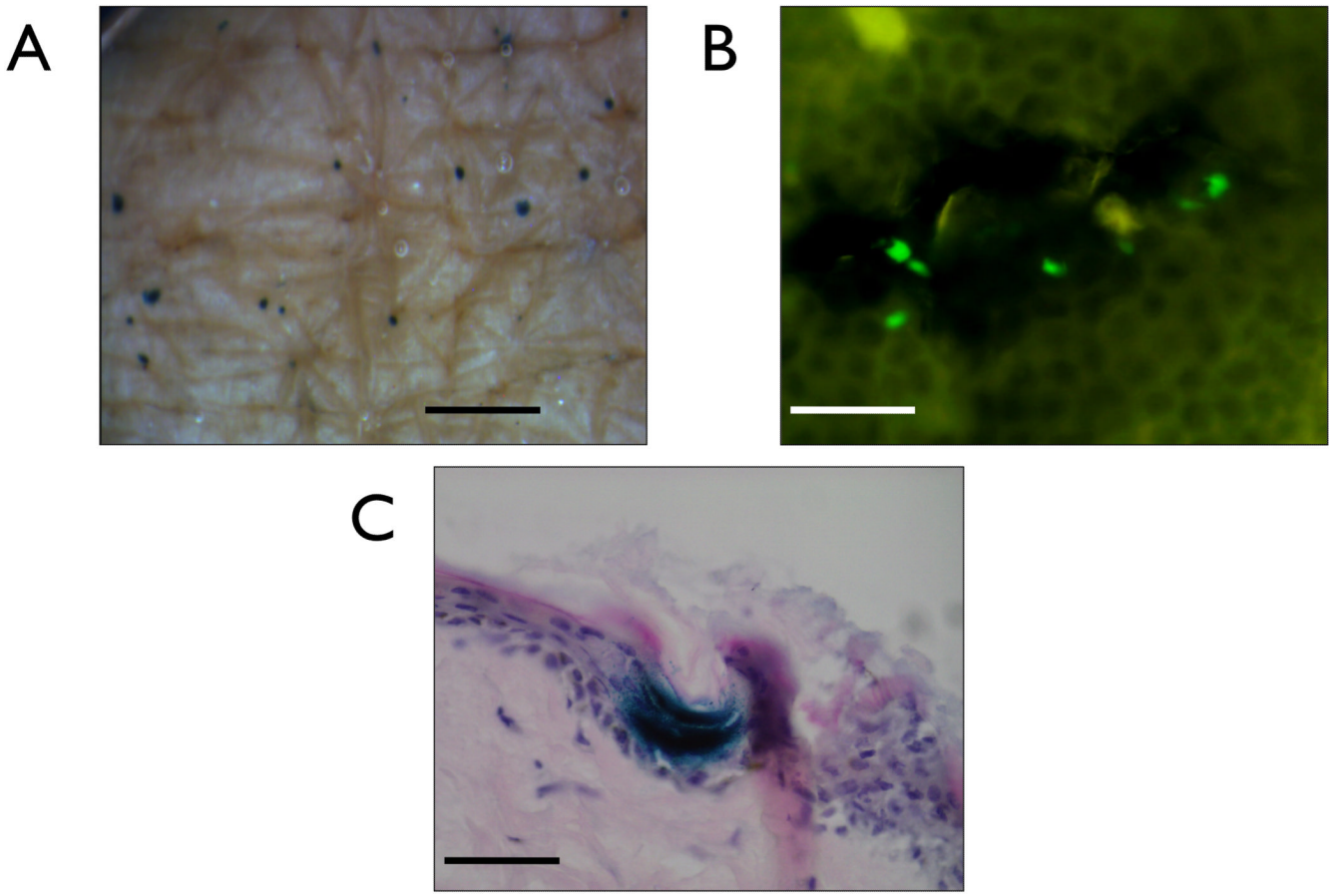

Figure 6. Positive gene expression from pDNA delivered as a liquid formulation via microneedles to viable human skin

(A) *En face* image showing positive points of gene expression resulting from multiple applications of the microneedle device through a pre-applied solution of plasmid encoding β-galactosidase and 24 hrs in organ culture (bar = 1mm). (B) A human epidermal sheet treated with a microneedles and a liquid formulation of plasmid encoding EGFP (bar = 50μm). (C) 10μm histological section showing positive gene confined to the epidermis (bar = 100μm).

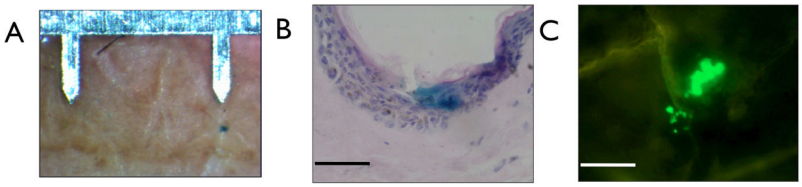

Figure 7. Positive gene expression from microneedle-coated pDNA delivered to viable human skin

(A) *En face* image of a single point of gene expression from a plasmid encoding β-galactosidase with the microneedle device as a scale reference. (B) A H&E stained 10 μm histological section of human skin showing the point of microneedle penetration and the positive gene expression from the delivered dry coated plasmid encoding β-galactosidase (bar = 100μm). (C) Human epidermal sheet treated with a microneedle device dry-coated with a plasmid encoding EGFP (bar = 100μm).

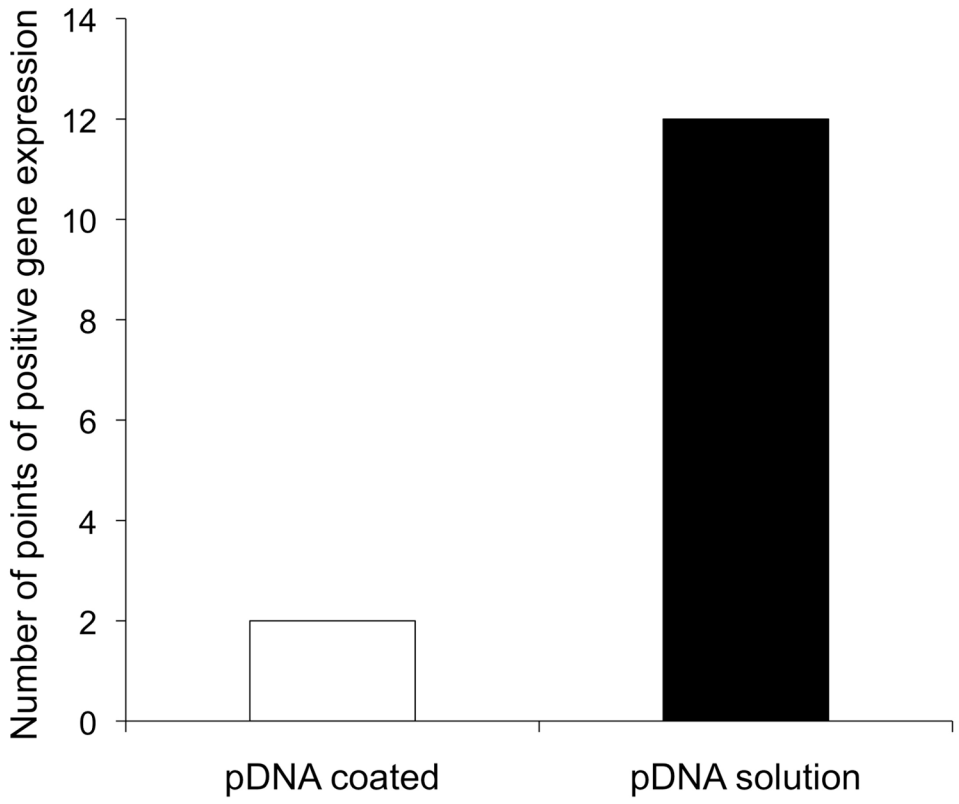

Figure 8. Differential levels in gene expression in human skin from pDNA delivered as a liquid formulation or as a dry-coated formulation

Data is total number of points of positive gene expression from three independent skin experiments. Significantly more discreet points of gene expression were observed in samples when pDNA was delivered as a solution compared to the coated formulation (Fishers exact test ($p= 0.0084$) $p < 0.01$).

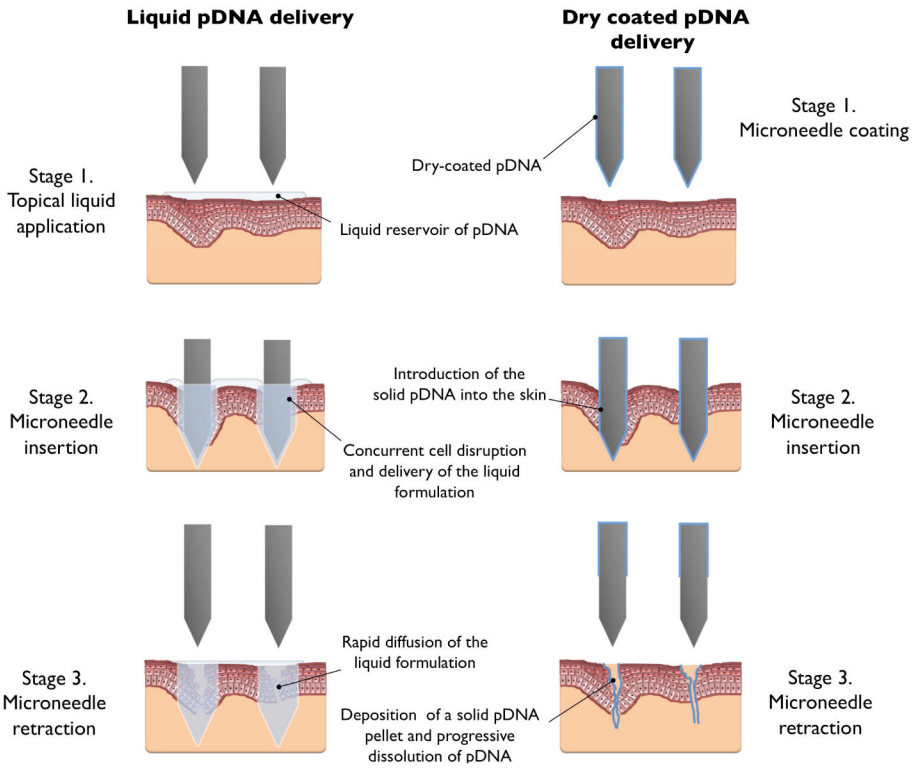

Figure 9.
A schematic highlighting the mechanisms of microneedle skin delivery for liquid-applied formulations and solid dry-coated formulations.